# ELECTROCHEMICAL BEHAVIOR OF LANTHANUM AND YTTRIUM IONS IN TWO MOLTEN CHLORIDES WITH DIFFERENT OXOACIDIC PROPERTIES: THE EUTECTIC LiCl-KCl AND THE EQUIMOLAR MIXTURE CaCl$_2$-NaCl

**Y. Castrillejo\*, M. R. Bermejo\*, A. M. Martínez\*\***

**and P. Díaz Arocas\*\*\***

\*Dpto de Química Analítica. Facultad de Ciencias. Universidad de Valladolid.
Prado de la Magdalena s/n. 47005 Valladolid Spain (E-mail: ycastril@qa.uva.es)
\*\*Department of Materials Technology, Sem Sælands vei 6, 7491 Trondheim, Norway
\*\*\*CIEMAT. Dept. de Fisión Nuclear. Avda. Complutense 22 Madrid 28040, Spain

## Abstract

*The electrochemical behavior of LaCl$_3$ and YCl$_3$ was studied in two molten chloride mixtures with different oxoacidic properties, the eutectic LiCl-KCl and the equimolar CaCl$_2$-NaCl melt at different temperatures. The stable oxidation states of both elements have been found to be (III) and (0) in both melts, and it was found that both La(III) and Y(III) cations were less solvated by the chloride ions in the calcium-based melt, which was explained by the stability of CaCl$_4^{2-}$ ions in that melt.*

*Transient electrochemical techniques, such as cyclic voltammetry, chronopotentiometry and chronoamperometry were used in order to study the reaction mechanism and the transport parameters of electroactive species at a tungsten electrode. The results showed that in the eutectic LiCl-KCl, the electrocrystallization of lanthanum and yttrium seems to be the controlling electrochemical step, while in CaCl$_2$-NaCl this phenomenon has not been observed. That was explained in terms of the differences in the physicochemical properties of the systems, especially interfacial tensions.*

*In the eutectic LiCl-KCl, chronoamperometric studies indicated instantaneous and three dimensional nucleation and crystal growth of lanthanum and yttrium whatever the applied overpotential of the rare earth metal is, whereas in the equimolar mixture $CaCl_2$-NaCl, the corresponding electrochemical exchanges were found to be quasi-reversible, and the values of the kinetic parameters, $K^0$ and $\alpha$, were obtained for both reactions.*

*Mass transport towards the electrode is a simple diffusion process, and the diffusion coefficients have been calculated. The validity of the Arrhenius law was also verified by plotting the variation of the logarithm of the diffusion coefficient versus 1/T.*

*Keywords:* molten chlorides, rare earths, lanthanum and yttrium chlorides, electrodeposition, nucleation and crystal growth, kinetic parameters

## 1. Introduction

During the last decades, molten salts and molten chlorides particularly have extensively proved to be suitable reaction media for performing selective solubilization or precipitation in chemical reactions, and have been already proposed as promising route for the treatment of raw materials. Moreover, electrochemical processes with metals (electrowinning, electrorefining, electroplating and electroforming) in molten salts media have extensively been proved to be more advantageous than those carried out in aqueous solutions. Higher efficiency of the electrolysis, lower energy consumption, often high electrodeposition rates and much better characteristics of the deposits [1] can be pointed out as some of the main advantages. The accumulated knowledge concerning their high-temperature electrochemistry allows the deposition of metals and their alloys. Those possibilities lie in the fact that, because of their variety, one can always find a solvent whose chemical and electrochemical characteristics and melting point are suitable to carry out the given process.

In the last years a new field has been developed - the use of molten salts media for pyrochemical separation as a promising option in the nuclear fuel technology in the future [2-8]. The interest is due to the progress in the assessment of new concepts for transmutation and the corresponding fuel cycles [9]. Today's main emphasis is put on the maximal cost reduction for cycle technology. In order to assess the feasibility of such pyrochemical separation, several processes have been developed for the recovery of minor actinides from spent metallic, nitride, oxide nuclear fuels, and high level radioactive liquid wastes [10, 11].

One of the most important steps in the pyrometallurgical reprocessing is the electrorefining from molten chlorides. In this step, spent metal fuel is anodically dissolved into molten chlorides, and the minor actinides are selectively recovered at the cathode due to the differences among the redox potentials of the elements, while fission products remain in the anode and/or in the electrolyte salt. The determination of thermodynamic data of solutions as well as the electrochemical behavior of the elements is of crucial

importance for the understanding of the process and the design of the separation cell.

The work presented here is a part of a wider project focused on the separation of actinides from rare earths – the most difficult fission product to separate due to their similar properties – from a simulated nuclear fuel (SIMFUEL). Hence, obtaining basic data of fission products in molten halogenide salts is the major concern. The work presents a study on the electrochemical properties of two rare earths, lanthanum and yttrium, trichlorides and has been carried out in two molten chlorides with different oxoacidity properties, the eutectic *LiCl-KCl* and the equimolar mixture *CaCl$_2$-NaCl*.

A few studies relating to the chemical behavior of lanthanum and yttrium in molten chlorides have been conducted. The eutectic *LiCl-KCl* and the equimolar mixture *NaCl-KCl* have been used for this kind of study [12-18]. It was Plambeck who systematized the standard potential values for a number of rare earths in the eutectic *LiCl-KCl* at 723 K [12], while the temperature dependence of these values were determined experimentally in [13-18].

The fundamental studies of the mechanism of electrode reactions in molten chlorides are, as yet, sparse. In the eutectic *LiCl-KCl* and *LiCl-KCl-NaCl* the electroreduction of lanthanum and yttrium trichlorides, at low concentration at solid cathodes such as *W*, seems to consist of only one electrochemical step, whose potential is close to the potential of the alkali metal electrodeposition [12, 17, 19]. The diffusion coefficients have been determined in works [17, 19-21], and some differences have been found.

It is known that rare earth metals are soluble in their molten chlorides [22-25] being responsible for the low current efficiency of the electrolysis, moreover, mixtures of rare earth chlorides and rare earth metals give rise to electronic conductivity, which may influence electrochemical measurements. The work of Keneshea and Cubbicciotti [25] indicates that the solubility of lanthanum in its liquid trichloride is 9% at 826 $^0$C and 11% at 914 $^0$C. Therefore, dilute solutions of *RECl$_3$* in the *LiCl-KCl* or *CaCl$_2$-NaCl* melts are expected to show very low metal solubility.

The purpose of our investigation was to determine the electrochemical behavior of lanthanum and yttrium ions in two molten chlorides with different intrinsic acidities, the eutectic *LiCl-KCl* melt at 723 K and the equimolar mixture *CaCl$_2$-NaCl* at 823 K, added as lanthanum and yttrium trichloride. Tungsten wires were utilized as working electrodes. Transient electrochemical techniques, such as cyclic voltammetry, chronopotentiometry and chronoamperometry, were used in order to study the reaction mechanism and the transport parameters of electroactive species. Moreover, nucleation studies of the rare earth metals in the eutectic mixture *LiCl-KCl* were carried out, something that, to our knowledge, is rarely found in the literature published so far. The results show under the experimental conditions the deposition of yttrium and lanthanum at a tungsten electrode can be explained in terms of a model involving instantaneous and three-dimensional nucleation, where the growth of the crystals is controlled by hemispherical or linear diffusion over the whole cathodic potential range studied.

## 2. Experimental

### 2.1. Preparation and purification of the melt

The experimental cell was carefully prepared. Therefore all handling of the salts was carried out in a glove box mBraun Labstar 50 under argon atmosphere. Moreover, purification of the cell was very important in order to obtain consistent results.

The chloride mixtures (*CaCl₂-NaCl* or *LiCl-KCl*, analytical grade) were melted in alumina or glassy carbon (GC) crucibles placed in a quartz cell inside a Taner furnace. A West 3300 programmable device controlled the temperature of the furnace to a precision of ±2 °C. The working temperature was measured with a thermocouple protected by an alumina tube inserted into the melt.

The mixture was fused under vacuum, then the pressure was raised to the atmospheric value using dry argon; afterwards it was purified by bubbling *HCl* through the melt for at least 30 min, and then kept under argon which removed the residual *HCl* and maintained inert atmosphere during experiments. This procedure has been used previously [26-31].

### 2.2. General features

Solutions of the electroactive species were prepared by direct additions of *RECl₃*. The experimental problems related to the low solubility of *LaOCl* and *Y₂O₃* prevented the preparation of stable solutions of *RE(III)* for longer periods, more than one day, and it was hard to know the exact amount of salt introduced into the melt; for that we bubbled *HCl* each day prior to determinations. The total concentration of dissolved rare earth was calculated by ICP-AES analysis of frequent melt samples.

### 2.3. Electrochemical apparatus and electrodes

Cyclic voltammetry and pulse techniques were performed with a PAR EG&G Model 273A potentiostat/galvanostat controlled by the PAR EG&G M270 software package.

The reference electrode consisted of a silver wire (1 mm diameter) dipped into a silver chloride solution (0.75 mol kg⁻¹) in the *CaCl₂-NaCl* or *LiCl-KCl* molten mixture placed in a Pyrex tube. Potentials were measured against the potential of the $Ag|AgCl$ couple and translated into potentials versus *Cl₂/Cl⁻* to make the comparison clear. The working electrode was a 1mm tungsten wire. Another tungsten wire was used as the counter electrode. The lower end of the tungsten electrode was polished thoroughly by using *SiC* paper. Then they were cleaned in ethanol using ultrasound followed by heating under vacuum. The active surface area of the working electrode was determined by measuring the depth of immersion.

Auxiliary techniques as SEM, X-ray diffraction analysis and ICP-MS analysis were also used.

## 3. Results and discussion

### 3.1. Voltammetric characterization of the electrochemical systems

The stable oxidation states of the studied rare earth elements, lanthanum and yttrium, were identified by different electrochemical techniques, i.e. cyclic voltammetry, chronopotentiometry and square wave voltammetry.

Figures 1(a-b) show some voltammograms obtained in the eutectic *LiCl-KCl* melt containing *RE(III)* ions at a tungsten electrode. The shape of the wave A, in the potential range close to the cathodic limit of the melt (electrodeposition of liquid lithium or sodium respectively) is characteristic of the formation of a new phase, steep rise and slow decay. The anodic peak A' has the expected characteristics for a stripping peak - the decay is steeper than the rise due to the depletion of the metal deposited during the forward scan. Moreover, the ratio of the forward to reverse current peaks $Ip^a/Ip^c$ is higher than unity.
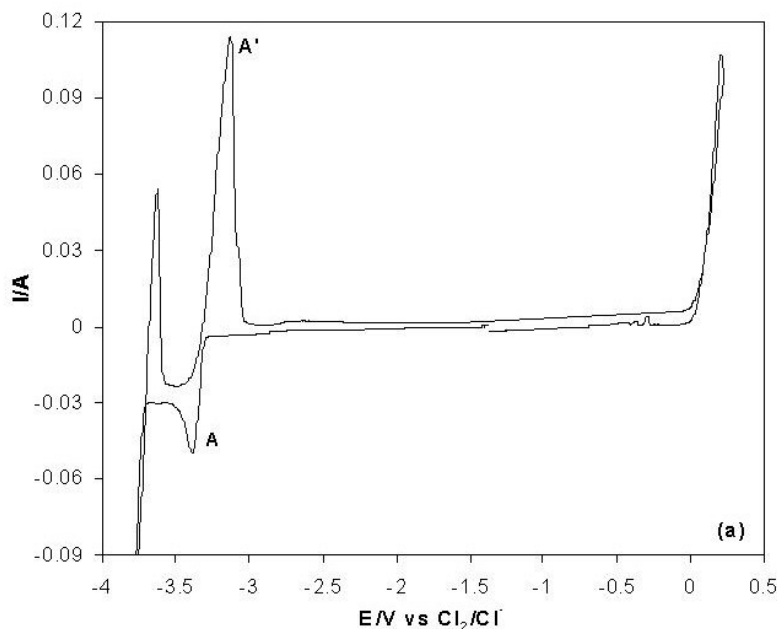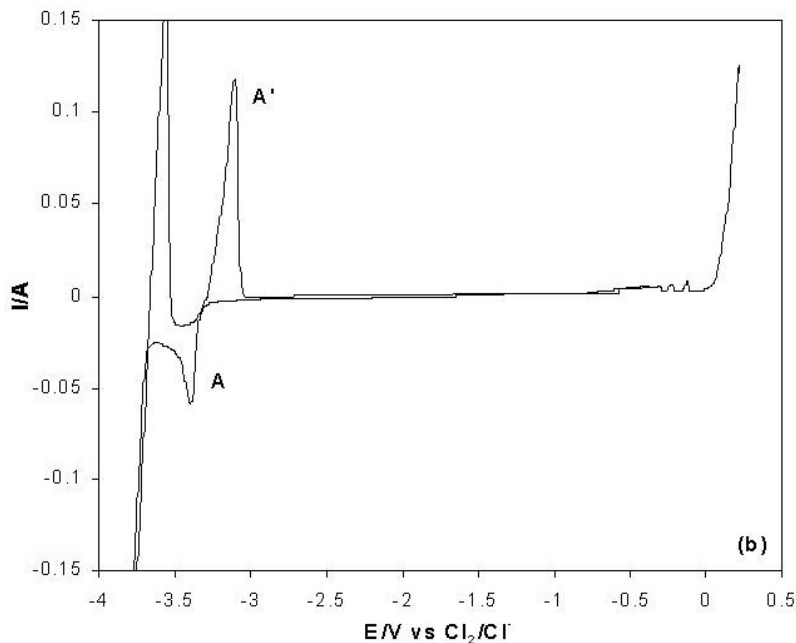
*Figure 1. a) Typical cyclic voltammogram for the reduction of lanthanum trichloride*
*(7.0955×10⁻⁵ mol cm⁻³) at a tungsten electrode (0.32 cm²) in the eutectic*
*LiCl-KCl melt at 723 K, sweep rate 0.2 V s⁻¹;*
*b) Cyclic voltammogram for the reduction of yttrium trichloride (8.8770×*
*10⁻⁵ mol cm⁻³) at a tungsten electrode (0.50 cm²) in the eutectic LiCl-KCl*
*melt at 723 K, sweep rate 0.2 V s⁻¹.*

In the case of the equimolar *CaCl₂-NaCl*, the voltammograms recorded show similar peaks (Fig. 2(a-b)). In agreement with the standard potential values obtained by us previously [18], the peak potentials for the deposition and dissolution of the metals are shifted towards less negative values. It can be explained in terms of lower cation complexation by the bath, probably due to the formation of the $CaCl_4^{2-}$ complex [33, 34], which leads to the decrease in free chloride ion concentration in the calcium melt in comparison with the molten *LiCl-KCl* mixture. In addition, a small oxidation wave B' (related to an inflection of the cathodic wave, B) is observed, which can be explained by the formation of a *RE-Na* alloy [35].

Square wave voltammograms were also obtained (Fig. 3). This technique was described in details by Osteryoung and Osteryoung [36], and Ramaley and Krasue [37].
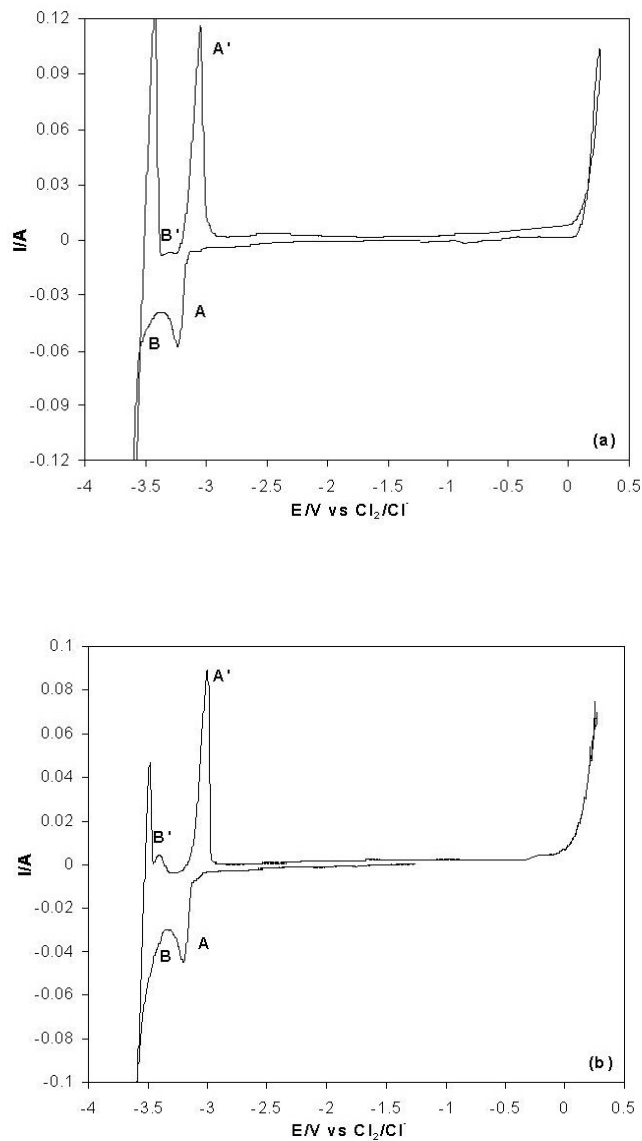
*Figure 2. a) Typical cyclic voltammogram for the reduction of lanthanum trichloride*
*(1.7008×10⁻⁴ mol cm⁻³) at a tungsten electrode (0.31 cm²) in the*
*equimolar CaCl₂-NaCl mixture at 823 K, sweep rate 0.2 V s⁻¹;*
*b) Cyclic voltammogram for the reduction of yttrium trichloride (1.6783×*
*10⁻⁴ mol cm⁻³) at a tungsten electrode (0.38 cm²) in the equimolar CaCl₂-*
*NaCl mixture at 823 K, sweep rate 0.2 V s⁻¹.*
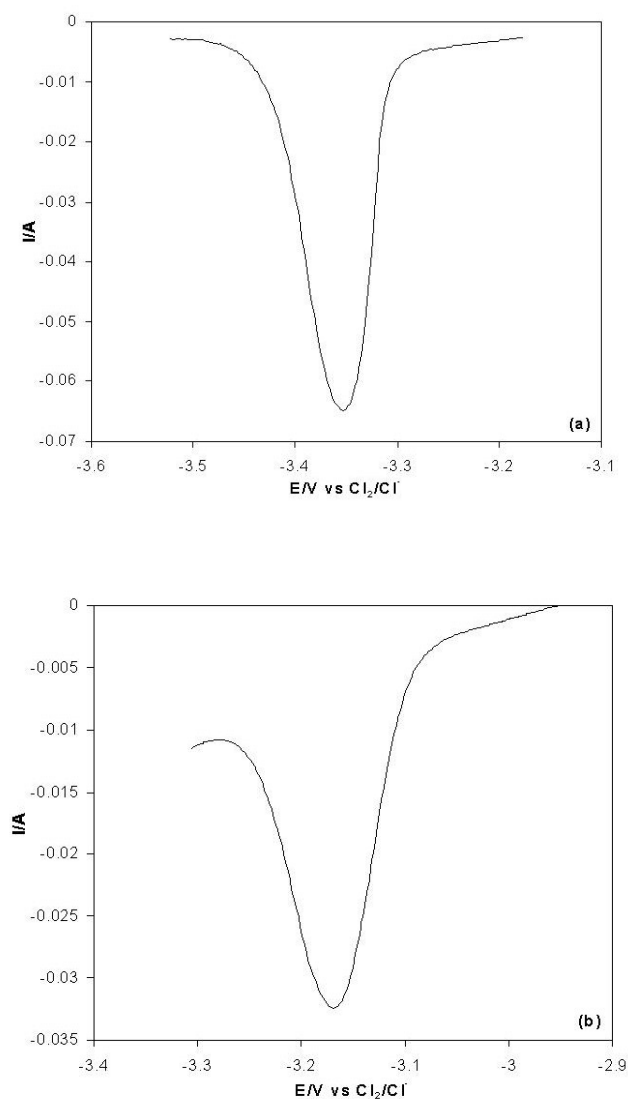
*Figure 3. a) Net-current square wave voltammogram for the reduction of Y(III) at a tungsten electrode in the eutectic LiCl-KCl melt at 723 K; pulse height: 25 mV; potential step: 1 mV; frequency: 50 Hz; A=0.44 cm²; b) Net-current square wave voltammogram for the reduction of La(III) at a  tungsten electrode in the eutectic CaCl₂-NaCl melt at 823 K; pulse height: 25 mV; potential step: 1 mV; frequency: 30 Hz; A=0.23 cm².*

The potential-time function consists of the sum of a synchronized square wave and a staircase potential ramp. The current is sampled at the end of every half wave and then differentiated. This allows capacitive and residual currents to be eliminated and makes the method highly sensitive. For a simple reversible reaction, the net current-potential curve is bell-shaped and symmetrical about the half-wave potential, and the peak height is proportional to the concentration of the electroactive species. The width of the half-peak, $W_{1/2}$, depends on the number of electrons exchanged and the temperature as follows:

$$W_{1/2} = 3.52 \frac{RT}{nF} \tag{1}$$

A single signal was obtained when sweeping in the negative direction, $W_{1/2}$ giving values of 3.0±0.2 electrons for lanthanum and yttrium.

Moreover, chronopotentiograms in both melts were obtained (see Figures 4(a-b)). The graphs indicate the existence of a potential plateau at approximately -3.3 and -3.2 V (vs. $Cl_2/Cl^-$). After this plateau there is a rapid decrease in the potential, and when the constant current was maintained for times longer than the transition time, the electrode potential reaches a limiting value corresponding to the deposition of the alkali metal (sodium or lithium). In the case of the calcium-based melts it is possible to observe the formation of the *RE-Na* alloy (zone B in the Figure 4b).
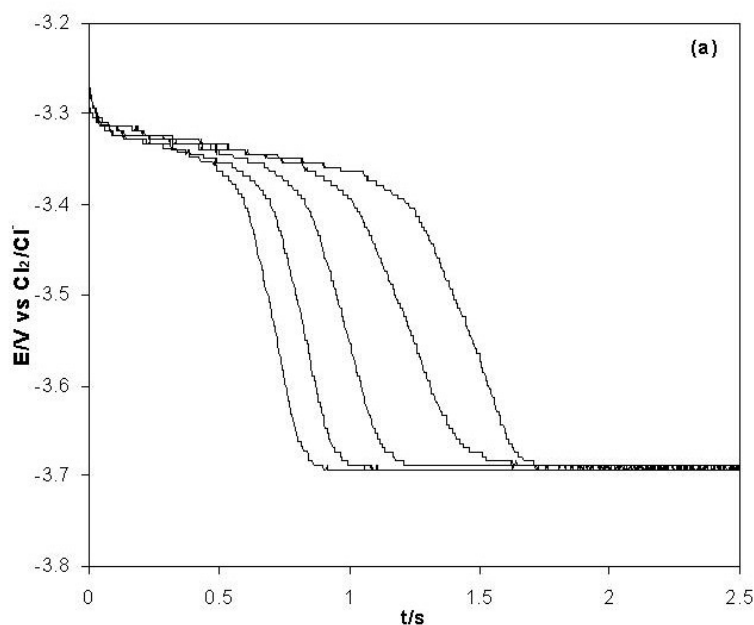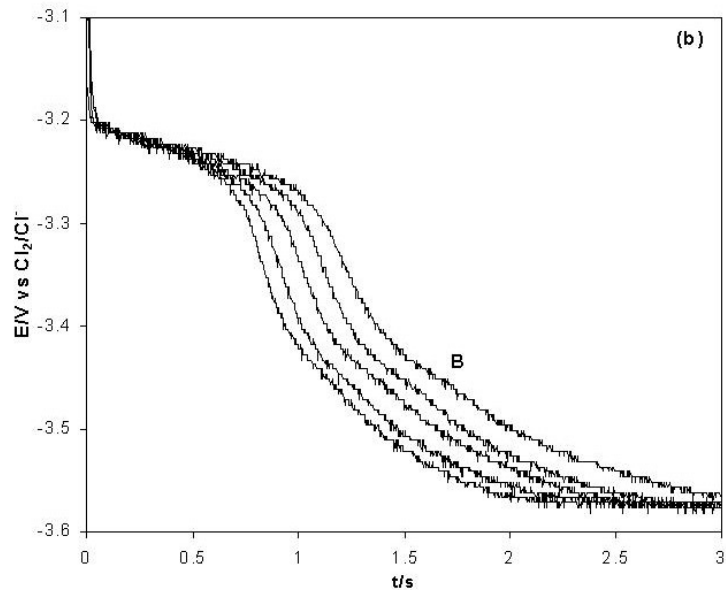
*Figure 4. a)Chronopotentiometric curves obtained on a tungsten electrode (0.34 cm$^2$) in the eutectic LiCl-KCl melt at 723 K containing LaCl$_3$ (9.5337×10$^{-5}$ mol cm$^{-3}$);*

*b)Chronopotentiometric curves obtained on a tungsten electrode (0.51 cm$^2$) in the equimolar CaCl$_2$-NaCl mixture at 823 K containing LaCl$_3$ (1.9723×10$^{-4}$ mol cm$^{-3}$).*

Analysis of the electrodeposits obtained by coulometry at controlled potential confirmed the formation of the metal. All these results show that the only stable oxidation states of lanthanum and yttrium in the melts studied are 0 and the dissolved *La(III)* and *Y(III)*.

### 3.2. Electrochemical nucleation of Y and La in the eutectic LiCl-KCl

#### 3.2.1. Results obtained by cyclic voltammetry

A typical cyclic voltammogram of *LiCl-KCl-RECl$_3$* at a tungsten electrode with the evidence of nucleation and crystal growth are shown in Fig. 5(a-b). A "crossover" of the direct and the reverse curve is visible in these voltammograms. The deposition of

yttrium and lanthanum does not commence until a potential well beyond $E_{rev}$ is reached. The reason for this behavior is that the formation of stable *RE* nuclei on an inert surface requires a potential more negative than the reduction of *La(III)* or *Y(III)* ions on a *La* or *Y* surface respectively. No evidence of UPD of *La* or *Y* on tungsten was observed.
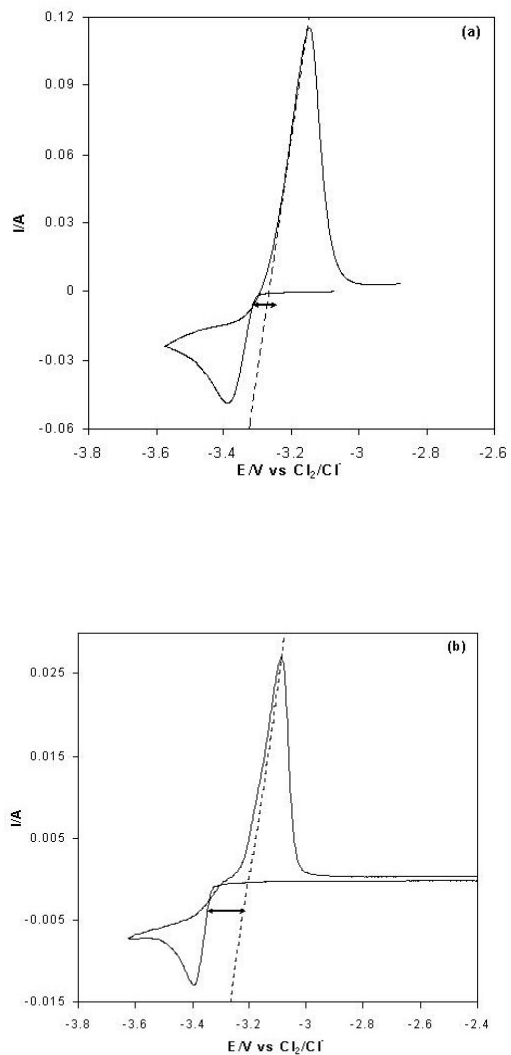


*Figure 5  Cyclic voltammograms illustrating the "nucleation crossover effect" on the return sweep for the deposition of: (a) lanthanum onto tungsten electrode; (b) yttrium onto tungsten electrode.*

### 3.2.2. Results obtained by chronoamperometry

Chronoamperometry is a technique particularly sensitive to nucleation and growth phenomena [38-42]. If the metal is deposited on a foreign substrate, the initial response of the current gives information about the nucleation behavior of the metal on the substrate.

*I-t* transients of *Y(III)* and *La(III)* for various potential pulses at a tungsten electrode are shown in Figures 6(a-b). The appearance of these curves indicated that nucleation and growth phenomena play a part in the overall deposition process. The initial regime of each transient is characterized by a decrease in current, which corresponds, after charging of the double layer, to the formation of the first nuclei. This is followed by an increase in the current associated with crystal growth on the electrode. Finally, the current decays in the usual way with time. The rising part of the current culminates in a maximum, $i_m$, as the individual diffusion zones of the growing nuclei merge, and we can see that the higher the overpotential, the greater the value of $i_m$. The position of this maximum on the time axis, $t_m$, depends on the magnitude of the potential step, and decreases as the applied potential becomes more negative.
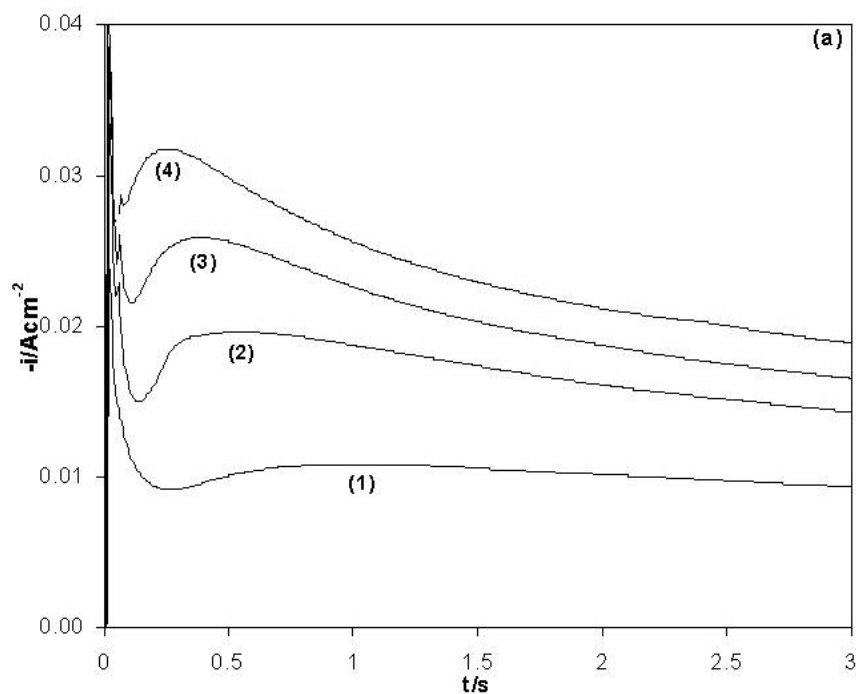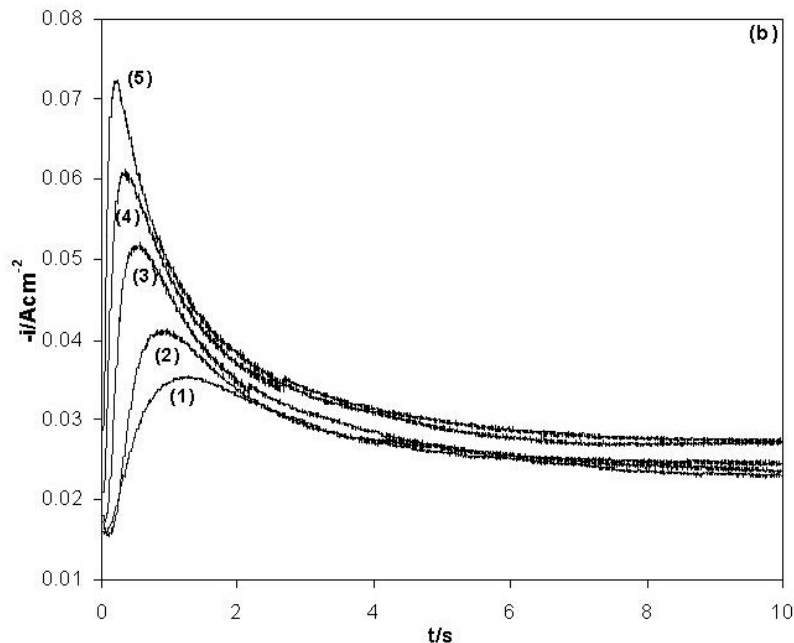
*Figure 6.  a) Potentiostatic current-time transients of LiCl-KCl-LaCl$_3$ at various over potentials [(1) -3.268, (2) -3.273, (3) -3.278 and (4) -3.283 V vs. Cl$_2$/Cl$^-$] with 9.534×10$^{-5}$ mol cm$^{-3}$ of LaCl$_3$ at a tungsten electrode (A=0.44 cm$^2$) at 723 K;*

*b) Potentiostatic current-time transients of LiCl-KCl-YCl$_3$ at various over potentials [(1) -3.275, (2) -3.281, (3) -3.287, (4) -3.290 and (5) -3.297 V vs. Cl$_2$/Cl$^-$] with 1.095×10$^{-4}$ mol cm$^{-3}$ of YCl$_3$ at a tungsten electrode (A=0.45 cm$^2$) at 723 K.*

After each run the deposited metal was removed from the surface by polarizing the working electrode anodically. The most interesting part of the cathodic *i-t* transients is the rising portion of the curve, which corresponds to the current before overlapping of the first monolayer of the growing nuclei and therefore can be used to determine the kinetics of nuclei growth. Then, the rising part of the chronoamperograms was analyzed and compared to models developed to describe instantaneous nucleation in which all the *RE* germs are created at the same moment at the beginning of the electrolysis; and progressive nucleation in which new crystals are continuously created throughout the electrolysis.

In order to identify the lanthanum and yttrium nucleation mode, we have analyzed: i) the relationship between current, *i*, and time, *t*; and ii) the non-dimensional plots of the chronoamperometric curves according to Scharifker et al [38].

According to the literature [38, 42], the relationship between current, *i*, and time *t*, at the beginning of the potential pulse is given by an equation of the following type: $i=\alpha t^x$. The exponent *x* depends on the type of nucleation, the geometry of the nuclei, and the growth conditions. Various models with corresponding values of $\alpha$ and x were presented by Allongue and Souteyrand [42].

The proportionality between *i* and $t^{1/2}$ (Figure 7) for various overvoltages demonstrates that initial stages of the electrochemical deposition of yttrium and lanthanum at a tungsten electrode can be explained in terms of a model involving instantaneous and three-dimensional nucleation. The growth of the crystals is controlled by hemispherical or linear diffusion [42].

Scharifker and Hills [38] developed a non-dimensional model adapted for this situation. Since the entire transient curve is analyzed, the non-dimensional model was found to be more accurate. The entire dimensionless experimental current-time transients obtained at different applied cathodic potentials were compared to the
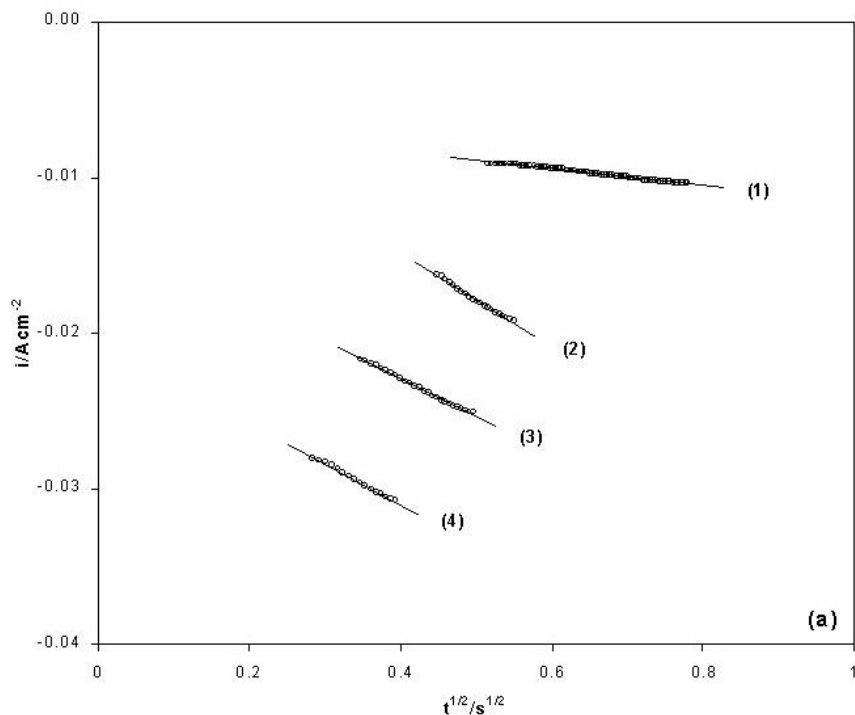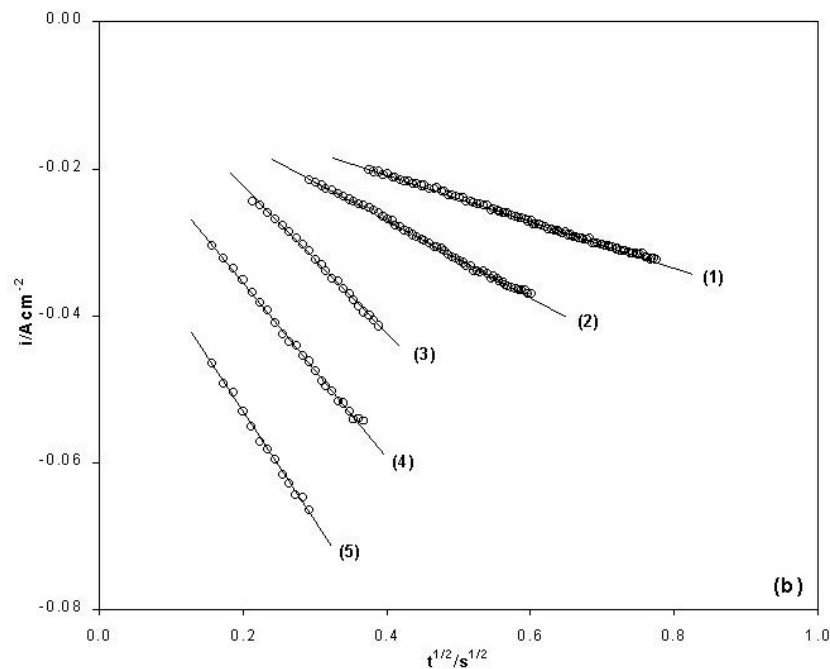
Fig. 7.Plots of i versus $t^{1/2}$ constructed from the rising portion of the curves shown in Figure 6 at various overpotentials: (a) Lanthanum: (1) -3.268, (2) -3.273, (3) -3.278 and (4) -3.283 V vs $Cl_2/Cl^-$ and (b) Yttrium: (1) -3.275, (2) -3.281, (3) -3.287,

appropriate theoretical transients reported by the authors for instantaneous and progressive nucleation (Equations (2) and (3) respectively).

$$\left(\frac{I}{I_{max}}\right)^2 = 1.9542 \frac{\left[1 - exp\left(-1.2564(t/t_{max})\right)\right]^2}{(t/t_{max})} \tag{2}$$

$$\left(\frac{I}{I_{max}}\right)^2 = 1.2254 \frac{\left[1 - exp\left(-2.3367(t/t_{max})^2\right)\right]}{(t/t_{max})} \tag{3}$$

The results (see Fig. 8) confirmed the above statement: initial stages of the electrochemical deposition of lanthanum and yttrium on a tungsten electrode in the eutectic

*LiCl-KCl* mixture can be explained in terms of a model involving instantaneous nucleation with three-dimensional growth of the nuclei.
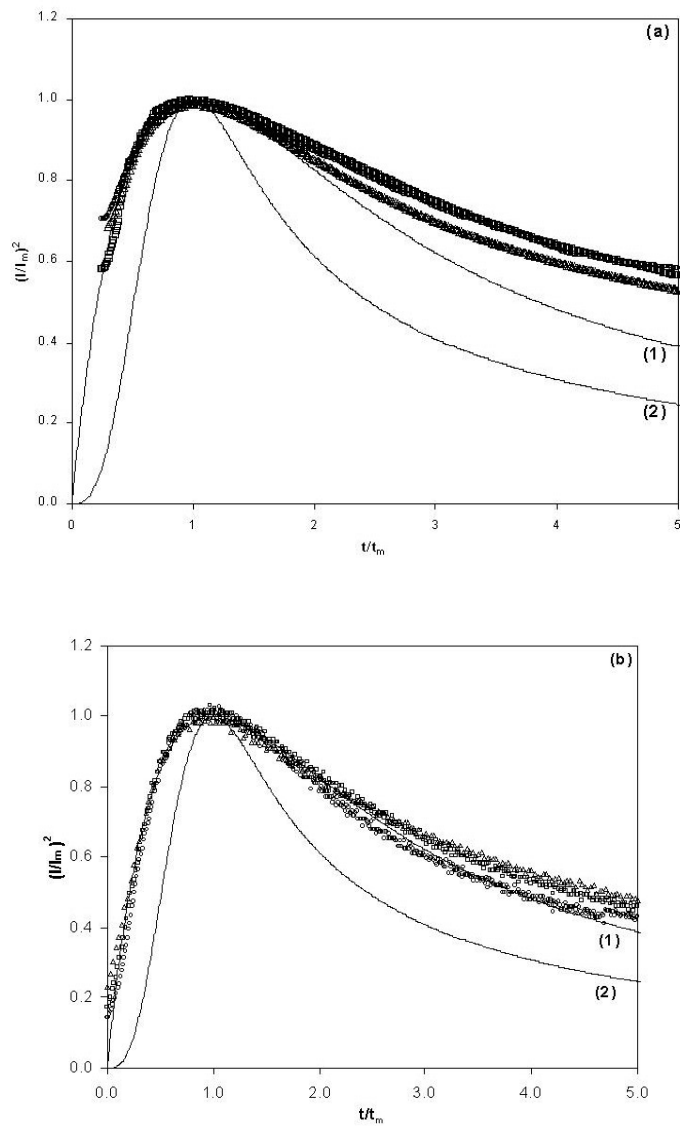


*Figure 8. Comparison of the dimensionless experimental data derived from the current-time transients with the theoretical models for (1) instantaneous and (2) progressive nucleation at different overvoltages: (a) Lanthanum: (o) -3.268, (□) -3.273 and (△) -3.278 V vs. $Cl_2/Cl^-$. (b) Yttrium: (o) -3.287, (□) -3.290 and (△) -3.297 V vs. $Cl_2/Cl^-$.*

### 3.3. Kinetics of the electrode reaction in the equimolar $CaCl_2$-NaCl. Reversibility studies

The characteristic crossover in the cathodic branch, whose presence indicates a large overpotential, was never observed in *La* and *Y* voltammograms in the calcium-based melt. Overall, the voltammetric peaks of the deposition and striping of these metals at tungsten are unremarkable in appearance. However, the voltammetric curves recorded at different sweep rates (Fig. 9(a-b)) clearly show that the peak potential $Ep^c$ shifts negatively, and the peak potential difference $Ep^c$-$E_{p/2}$ increases when the sweep rate is increased. This fact suggests under these conditions and after correction of the ohmic drop, the electron transfer rate is significantly lower than that of the mass transport [43-45].

An alternative approach to the interpretation of the mechanism and the estimation of kinetic parameters is the convolutional analysis of the voltammetric curves [46-50]. Figure 10 shows some voltammograms of *RE(III)* reduction and their corresponding semi-integral curves. Analyzing the convoluted curves, we can observe that the direct and reverse scans are not identical and hysteresis behavior occurs between the upper and downer sweeps. All these characteristics support the fact that the reduction of *La(III)* and *Y(III)* at a *W* electrode is not reversible.

Logarithmic analysis of the convoluted curves, according to the model of a quasi-reversible exchange with the formation of an insoluble product, was carried out applying the equation [51-53]:

$$E = E_1^o + 2.3 \frac{RT}{\alpha nF} \log k^o + 2.3 \frac{RT}{\alpha nF} \log B \qquad (4)$$

$$B = \frac{(m^* - m)D^{-1/2} + nFA \exp\left[ (nF/RT)(E - E_1^o) \right]}{I} \qquad (5)$$

where *m* is the convoluted current, $m^*$ its limiting value, *A* the active surface area of the electrode, and $E_1^O$ the standard potential of the *RE(III)/RE(0)* couple previously obtained by us by potentiometry [18].

Plots of *E* vs. log *B* (see Fig. 10) were a straight line, from whose slope and intercept one can extract the value of the transfer coefficient, $\alpha$, and the charge-transfer rate constant, $k^o$, respectively. The average values obtained in this way are given in Table 1.

Taking into account the Matsuda and Ayabe criteria [54], in which the charge-transfer rate constant and the sweep rate are related, it can be confirmed that the *La(III)/La(0)* and *Y(III)/Y(0)* reactions are quasi-reversible at a tungsten electrode.
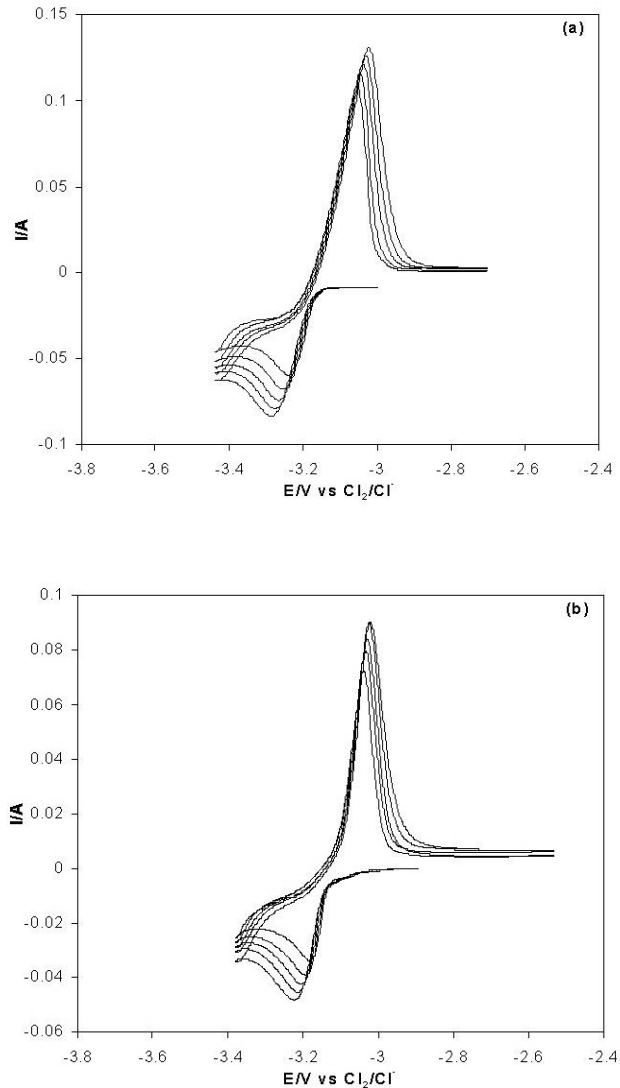
*Fig. 9. a) Variation of the voltammograms for the reduction of lanthanum*
*trichloride (1.7000x10$^{-4}$ mol cm$^{-3}$) with the sweep rate. Tungsten*
*electrode (0.31 cm$^2$). Equimolar CaCl$_2$-NaCl mixture at 823 K. Sweep*
*rates: 0.2; 0.3; 0.4; 0.5 and 0.6 V s$^{-1}$.*
*b) Variation of the voltammograms for the reduction of yttrium trichloride*
*(1.6783x10$^{-4}$ mol cm$^{-3}$) with the sweep rate. Tungsten electrode (0.21 cm$^2$).*
*Equimolar CaCl$_2$-NaCl mixture at 823 K. Sweep rates: 0.2; 0.3; 0.4; 0.5*
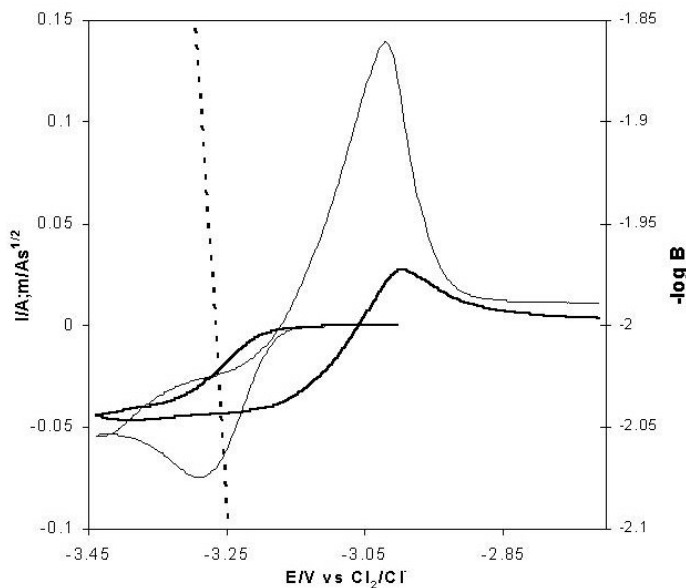*and 0.6 V s$^{-1}$.*

*Fig. 10. Voltammogram for the reduction of lanthanum trichloride on a tungsten electrode, their corresponding convolution curve (gross lines) and the logarithmic analysis of the convoluted data (-----) following a quasire versible model. Equimolar CaCl$_2$-NaCl mixture at 823 K. c$_0$ =1.7000x10$^{-4}$ mol cm$^{-3}$; A = 0.31 cm$^2$). Sweep rates: 0.6 V s$^{-1}$.*

*Table 1.- Values of the kinetic parameters, k$^o$ and α, corresponding to the La(III)/La(0) and Y(III)/Y(0) electrochemical systems in the equimolar mixture CaCl$_2$-NaCl at 823K*

| Rare earth | log k$^o$, cm s$^{-1}$ | α |
|------------|------------------------|---|
| La | -3.9 ± 0.1 | 0.48 ± 0.03 |
| Y | -3.7 ± 0.2 | 0.39 ± 0.05 |

Under the given experimental conditions (diluted *RE(III)* solutions), we have not observed by the *I-t* current transients that the nucleation and growth phenomena step controls the overall *RE* electrodeposition process in this melt. Thus, one can say that it is probably the charge transfer step, which controls the process, rather than nucleation and growth.

### 3.4. Determination of the RE(III) diffusion coefficient. Verification of the Arrhenius law

The diffusion coefficients, $D_{RE(III)}$, given in Table 2, were calculated from different electrochemical techniques by applying the appropriate equations. It has to be indicated that, although a tungsten wire was used as working electrodes, all the formulas used are relevant to plane semi-infinite diffusion because, under the experimental conditions, the

*Table 2.- Diffusion coefficients of La(III) and Y(III) calculated by different electro chemical techniques*

| Electrochemical Technique | LiCl-KCl at 723 K $10^5 \cdot D$, cm$^2$ s$^{-1}$ | | CaCl$_2$-NaCl at 823 K $10^5 \cdot D$, cm$^2$ s$^{-1}$ | |
|---|---|---|---|---|
| | La(III) | Y(III) | La(III) | Y(III) |
| Semi-Integral | 1.15±0.12 | 1.00±0.10 | 0.95±0.10 | 0.90±0.01 |
| Chronopotentiometry | 1.17±0.13 | 0.93±0.12 | 0.97±0.12 | 0.87±0.03 |

corrections related to cylindrical geometry can be neglected [55-58].

Chronopotentiometric studies of the reduction of *RE(III)* ions obeyed the Sand's law [44]:

$$I\tau^{1/2} = \frac{nFAc_oD^{1/2}\pi^{1/2}}{2}$$

(6)

Transition times for several current densities were measured and the resulting $I$ versus $1/\tau^{1/2}$ plot yielded a straight line, indicating that the fluxes of *RE(III)* species were diffusion controlled (see Fig. 11). From the slope of the plot it was possible to determine the diffusion coefficient of *RE(III)* ions.
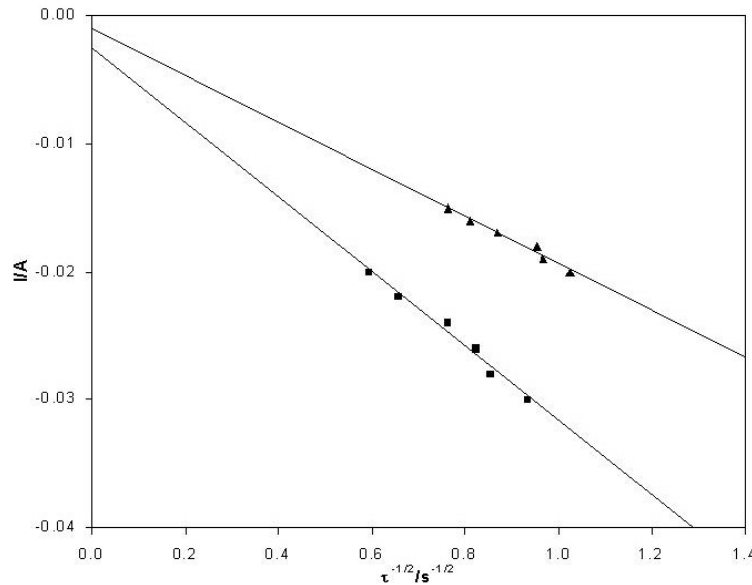


*Figure 11. Verification of the Sand′s law. Data obtained from the chronopotentiometric curves obtained from Figure 3. (■) Eutectic LiCl-KCl melt at 723 K. (▲) Equimolar CaCl$_2$-NaCl mixture at 823 K.*

The convoluted curves of the voltammograms exhibited relatively well defined limiting currents (see Figs. 10 and 12), indicating that there is no gross change in the electrode surface area during the scan, to the point that it affects the limiting current for the *RE(III)* reduction wave. Then the *RE(III)* diffusion coefficient was computed from the boundary semi-integral values by means of the relationship [44]:

$$m^* = nFAc_oD^{1/2} \tag{7}$$

It could also be interesting to study the variation of the transport properties of the *RE(III)* ions in the melts with the temperature. Chronopotentiometric curves of *RE(III)* solutions were obtained when the working temperature was varied from 673 to 823 K and from 823 to 923 K in the eutectic *LiCl-KCl* melt and the equimolar *CaCl$_2$-NaCl* respectively.

The diffusion coefficients were determined from the chronopotentiometric curves by applying Eq. (6). Fig. 13 shows the variation of the logarithm of the diffusion coefficient versus *1/T*. Straight lines obtained show the validity of the Arrhenius law. From the equations of the plots obtained (Table 3) the temperature dependence of the diffusion coefficient was established, and the activation energy value for the diffusion process could be extracted.
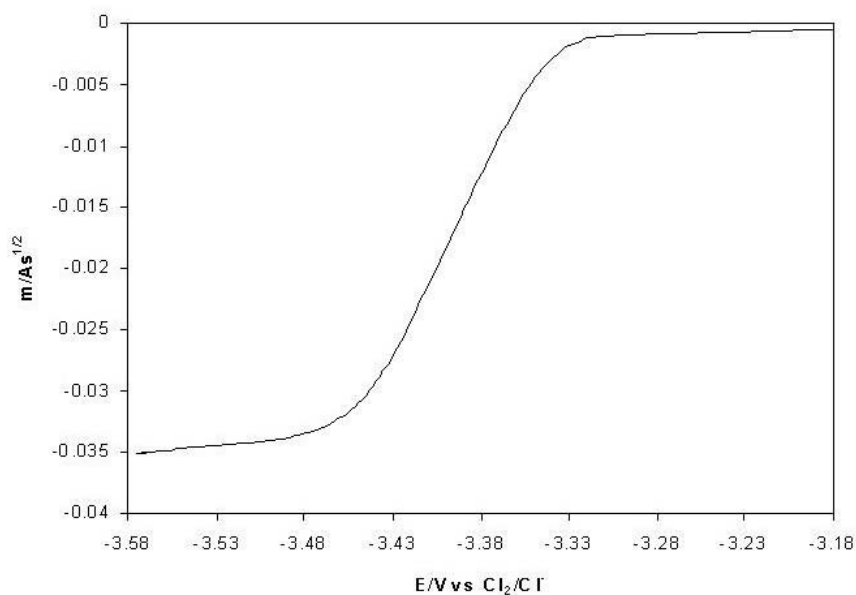


*Fig. 12. Convoluted curve of the voltammogram obtained for the reduction of lanthanum trichloride on a tungsten electrode. $c_0 = 8.0835 \times 10^{-5}$ mol cm$^{-3}$; $A = 0.44$ cm$^2$. Eutectic LiCl-KCl at 723 K. Sweep rates: 0.4 V s$^{-1}$.*

Although, as stated above, *RE(III)* cations are less solvated by the chloride ions in the calcium-based melt, the diffusion coefficient estimated shows that *RE(III)* diffuse more slowly in the equimolar *CaCl$_2$-NaCl* than in the eutectic *LiCl-KCl*. This behavior can be explained by different viscosity of the two media, which significantly reduce the mobility of *RE(III)* in the *CaCl$_2$-NaCl* melt.
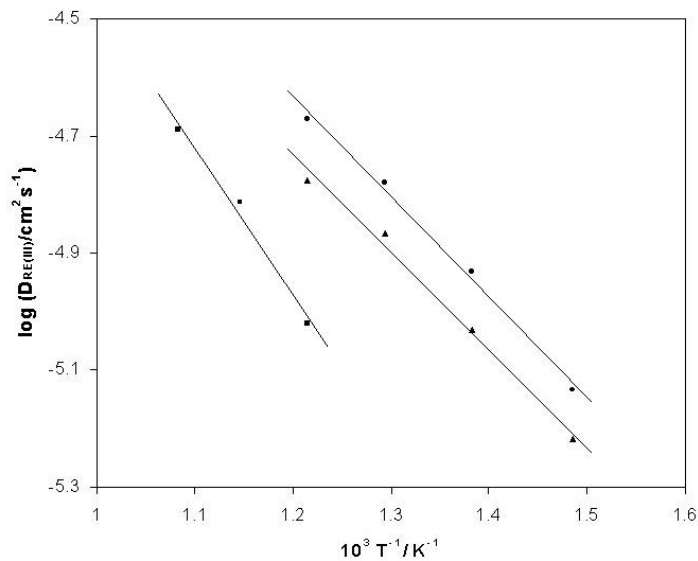
*Figure 13. Verification of the Arrhenius law. (●) LaCl₃ in the eutectic LiCl-KCl melt. (■) YCl₃ in the eutectic LiCl-KCl melt. (▲) LaCl₃ in the equimolar CaCl₂-NaCl mixture.*

*Table 3. Variation of the diffusion coefficient of La(III) and Y(III) ions with the temperature and activation energy of the diffusion process in the eutectic LiCl-KCl*

| Ion | Molten chloride | Equation $\log D_{RE(III)} = A + B\dfrac{1000}{T}$ | | $\Delta H$, kJ mol$^{-1}$ |
|---|---|---|---|---|
| | | $A$ | $B$ | |
| La(III) | LiCl-KCl | -2.57 | -1.717 | 32.86 |
| | CaCl₂-NaCl | -2.09 | -2.405 | 46.04 |
| Y(III) | LiCl-KCl | -2.73 | -1.669 | 31.94 |

## 4. Conclusions

The electrochemical properties of lanthanum and yttrium have been studied using tungsten as working electrode in two molten chloride mixtures with different oxoacidic properties - the eutectic *LiCl-KCl* at 723 K and the equimolar *CaCl₂-NaCl* melt at 823 K - founding some differences in behavior of the two chloride mixtures.

The cathodic peak potential values of the *RE(III)/RE* electrochemical exchange were less negative in the case of the calcium-based melt, which could be explained by a lower cation complexation in such melts due to the formation of the $CaCl_4^{2-}$ complex, which leads to the decrease in free chloride ions concentration than in the case of the molten eutectic *LiCl-KCl* mixture. The standard potential values of the different electrochemical exchanges and the activity coefficient values of the *RECl₃* species obtained in both melts and reported elsewhere also support this fact.

By combining different electrochemical techniques (i.e. voltammetry, chronopotentiometry and square wave voltammetry), it was possible to determine the stable oxidation states of lanthanum and yttrium in the molten chloride mixtures. Then, the stability of the rare earth metals was demonstrated in both melts, and their solubility in the molten chloride containing *RE(III)* ions was considered to be negligible. No UPD of metallic lanthanum and yttrium on tungsten substrates was found, and possible formation of *RE-Na* alloys was evidenced in the calcium-based melts.

Voltammetric and chronoamperometric techniques showed that the nucleation and growth of the metallic lanthanum and yttrium deposit show an important role in the overall electrodeposition process in the case of the molten eutectic *LiCl-KCl* mixture. The analysis of the transient curves (both of the rising part and the complete curve according to a non-dimensional model) showed that the initial stages of electrochemical deposition of lanthanum and yttrium at a tungsten electrode can be explained in terms of a model involving instantaneous nucleation (i.e. all the nuclei are formed "immediately" after applying the potential step) with three-dimensional growth of the nuclei. Identical results were found when varying the working temperature from 673 to 823 K.

However, in the case of the equimolar *CaCl₂-NaCl* melt at 823 K it was found that it is the charge transfer step, which controls the electrodeposition process, rather than nucleation and growth. The values of the charge transfer constant, $k^o$, calculated by logarithmic analysis of the convoluted voltammetric curves, showed a quasi-reversible behavior of the systems.

Moreover, the diffusion coefficients of the *RE(III)* ions were obtained by different electrochemical techniques (i.e. convolution and chronopotentiometry), and they showed a temperature dependence according to the Arrhenius law in both melts. It could be expected that some of the values obtained are somehow influenced by the alkali metal co-deposition, especially in the *CaCl₂-NaCl* melt.

In addition, the obtained diffusion coefficient values show that, although *RE(III)*

cations are less solvated by the chloride ions in the *CaCl₂-NaCl* melt, they are found to diffuse slower than in the eutectic *LiCl-KCl* at 723 K. That is probably due to higher viscosity of the calcium-based melt, which significantly reduce the mobility of *RE(III)* chlorocomplexes.

### Acknowledgements

### References

1. R.S. Sheti, J. Appl. Electrochem., 9 (1979) 411.
2. T. Koyama, M. Iizuka, H. Tanaka, M. Tokiwai, Y. Shoji, R. Fujita and T. Kobayashi, J. Nucl. Sci. Technol., 34 (1997) 384.
3. T. Nishimura, T. Koyama, M. Iizuka and T. Tanaka, Progress in Nuclear Energy, 32 (3/4) (1998) 381-387.
4. J.J. Laidler, Proc. AIP Conference on Accelerator Driven Transmutation Technologies and Applications, Las Vegas, Nevada, USA, 1994.
5. T.H. Pigford, An Invited Review for the MIT International Conference on the Next Generation of Nuclear Power Technology, Department of Nuclear Engineering, University of California at Berkeley, CA, UCB-NE-4176, Rev. 1 (Oct. 5, 1990).
6. K. Kinoshita, T. Inoue, S.P. Fusselman, D.L. Grimmett, J.J. Roy, R.L. Gay, C.L. Krueger, C.R. Nabelek and T. S. Storvick, J. Nucl. Sci. Technol., 36 (1999) 189.
7. Y.I. Chang, Nucl. Technol., 88 (1989) 129-138.
8. J.P. Ackerman, Proc. AIP Conference on Accelerator Driven Transmutation Technologies and Applications, Las Vegas, Nevada, USA, 1994.
9. Actinide and Fission Product Partitioning and Transmutation. Status and Assessment report. NEA/OCDE, 1999.
10. Y. Sakamura, T. Inoue, O. Shirai, T. Iwai, Y. Arai and Y. Suzuki, Proc. Global'99 Conference, Jackson Hole, Wyoming, USA, 1999.
11. J.J. Laidler, Transactions of the American Nuclear Society (USA), 68 (1993) 16-17. Proc. American Nuclear Society (ANS) Annual Meeting, San Diego, California, USA, 1993.
12. J.A. Plambeck, in Encyclopaedia of Electrochemistry of the Elements, Volume X: "Fused Salt Systems" (A. J. Bard), Marcel Dekker, New York, 1976.
13. L. Yang and R.G. Hudson, Trans Met. Soc. AIME, 259 (1959) 589.
14. J.J. Roy, L.F. Grantham, L.R. McCoy, C.L. Krueger, T. Storvick, T. Inoue, H. Miyashiro and N. Takahashi, Mater. Sci. Forum, 73-75 (1991) 547.

15. S.P. Fusselman, J.J. Roy, D.L. Grimmett, L.F. Grantham, C.L. Krueger, C.R. Nabelek, T.S. Storvick, T. Inoue, T. Hijikata, K. Kinoshita, Y. Sakamura, K. Uozumi, T. Kawai and N. Takahashi, J. Electrochem. Soc., 146 (1999) 2573.
16. Y. Mottot, Ph.D. thesis, Paris, 1986.
17. F. Lantelme, T. Cartailler, Y. Berghoute and M. Hamdani, J. Electrochem. Soc., 148 (9) (2001) C604-C613.
18. Y. Castrillejo, M.R. Bermejo, E. Barrado, A.M. Martínez and P. Díaz Arocas, J. Electroanal. Chem., Submitted for publication.
19. Y. Ito, Proc. International Symposium on Molten Salts and Technology, The Electrochem. Soc., 93-9 (1993) 240-251.
20. M.V. Smirnov, Yu.N. Krasnov, V.E. Komarov and V.N. Alekseev, in Transactions of the Institute of Electrochemistry, Urals Academy of Sciences, 6 (1968) 47.
21. G.S. Picard, Y.E. Mottot and B.L. Trémillon, Proc. IV International Symposium on Molten Salts, The Electrochem. Soc., 84-2 (1984) 585-602.
22. G.W. Mellors and S. Senderoff, J. Phys. Chem., 63 (1959) 1959.
23. L.F. Druding and J. D. Corbett, J. Am. Chem. Soc., 83 (1961) 2462.
24. L. Feng, Ch. Guo and D. Tang, J. of Alloys and Compounds, 234 (1996) 183-186.
25. F.H. Keneshea, Jr and D. Cubicciotti, J. Chem. Eng. Data, 6 (1961) 507.
26. F. Seon, Ph.D. thesis, Paris, 1981.
27. G. Picard, F. Seon and B. Tremillon, J. Electroanal. Chem., 102 (1979) 65.
28. A.M. Martínez, Ph.D. thesis, Valladolid, 1999.
29. A.M. Martínez, Y. Castrillejo, E. Barrado, G.M. Haarberg and G. Picard, J. Electroanal. Chem., 449 (1998) 67.
30. F. Seon, G. Picard and B. Tremillon, Electrochim. Acta, 28 (1983) 209.
31. Y. Castrillejo, A.M. Martínez, G.M. Haarberg, B. Børresen, K.S. Osen and R. Tunold, Electrochim. Acta, 42 (1997) 1489.
32. Y. Castrillejo, M.R. Bermejo, R. Pardo and A.M. Martínez, J. Electroanal. Chem. 522 (2002) 124-140.
33. K. Igarashi, T. Nijima and J. Mochinaga, Proc. I International Symposium on Molten Salt Chemistry and Technology, 1983, p. 469.
34. V.G. Roewer and H.H. Emons, Z. Anorg. Allg. Chem., 370 (1969) 128.
35. S. Thörnblad, Diploma work, Department of Materials Technology and Electrochemistry, NTNU, Trondheim, Norway, 1997.
36. J. Osteryoung and R.A. Osteryoung, Anal. Chem., **57** (1985) 101.
37. L. Ramaley and M.S. Krasue, Anal. Chem., 41 (1969) 1362.
38. B. Scharifker and G. Hills, Electrochim. Acta, 28 (1983) 879.
39. G. Gunawardena, G. Hills, I. Montenegro and B. Scharifker, J. Electroanal. Chem., 138 (1982) 225.
40. K. Serrano and P. Taxil, J. Appl. Electrochem., 29 (1999) 505-510.
41. P. Chamelot, B. Lafage and P. Taxil, J. Electrochem. Soc., 143 (5) (1996) 1570-1576.

42. P. Allongue and E. Souteyrand, J. Electrochem. Soc., 139 (1992) 5.

43. G. Mamantov, D.L. Manning, J.M. Dale, J. Electroanal. Chem., 9 (1965) 253.

44. A.J. Bard and L.R. Faulkner, Electrochemical Methods: Fundamentals and Applications, J. Wiley and Sons, New York, 1980.

45. Instrumental Methods in Analytical Chemistry, Southampton Electrochemistry Group, Ellis Horwood, Chichester, 1990.

56. J.C. Imbeaux and J.M. Savéant, J. Electroanal. Chem., 44 (1973) 169.

47. J.M. Savéant and D. Tessier, J. Electroanal. Chem., 61 (1975) 251.

48. K.B. Oldham, Anal. Chem., 44 (1972) 196.

49. M.G. Goto and K. Oldham, Anal. Chem., 45 (1973) 2043-2049.

50. J.C. Myland and K. Oldham, Anal. Chem., 66 (1994) 1866-1872.

51. Y. Castrillejo, A.M. Martínez, M. Vega, E. Barrado and G. Picard, J. Electroanal. Chem., 397 (1995) 139.

52. M. Mohamedi, Ph.D. thesis, Grenoble, 1995.

53. M.P. Quintana, Ph.D. thesis, Paris, 1993.

54. H. Matsuda and Y. Ayabe, Z. Electrochem., 59 (1955) 494.

55. Z. Galus, Fundamentals of Electrochemical Analysis, second (revised) edition, Ellis Horwood, Chichester, and Polish Scientific Publishers, PWN, Warsaw, 1994.

56. D.G. Peters and J.J. Lingane, J. Electroanal. Chem., 2 (1961) 1.

57. K.B. Oldham, J. Electroanal. Chem., 41 (1973) 351.

58. D.H. Evans and J.E. Price, J. Electroanal. Chem., 5 (1963) 77.